Journal of the Korean Society of Surveying, Geodesy, Photogrammetry and Cartography
Vol. 32, No. 1, 1-8, 2014
http://dx.doi.org/10.7848/ksgpc.2014.32.1.1

ISSN 1598-4850(Print)
ISSN 2288-260X(Online)
Orignal article

Three Line Scanner의 초점거리 오차의 영향에 관한 연구

Analysis of the Effects of Three Line Scanner's Focal Length Bias

김창재[1)]
Kim, Changjae

Abstract

The positions, attitudes, and internal orientation parameters of three line scanners are critical factors in order to acquire the accurate location of objects on the ground. Based on the assumption that positions and attitudes of the sensors are derived either from direct geo-referencing which of using Global Positioning Systems (GPS) and Inertial Navigation Systems (INS), or from indirect geo-referencing which of using Ground Control Points (GCPs), this paper describes on biased effects of Internal Orientation Parameter (IOP) on the ground. The research concentrated on geometrical explanations of effects from different focal length biases on the ground. The Synthetic data was collected by reasonable flight trajectories and attitudes of three line scanners. The result of experiments demonstrated that the focal length bias in case of indirect geo-referencing does not have critical influences on the quality of reconstructed ground space. Also, the relationships between IO parameters and EO parameters were found by the correlation analysis. In fact, the focal length bias in case of the direct geo-referencing caused significant errors on coordinates of reconstructed objects. The RMSE values along the vertical direction and the amount of focal length bias turned out to be almost perfect linear relationship.

Keywords : Three line scanner, Focal length bias, Direct and indirect geo-referencing

1. Introduction

The main purpose of photogrammetric field is to reconstruct object space accurately (Fraser *et. al.*, 2002; Lee and Bethel, 2004). To achieve the purpose, processes to determine the interior and exterior orientation parameters of cameras (or sensors) are significant. The interior orientation determines internal characteristics of a sensor and parameters, such as focal length, principal point, lens distortion, while the exterior orientation's parameters include a position and an attitude of the sensor. Sensors, mounted on the crafts (i.e., space-born or air-borne crafts), are calibrated in the laboratory before launching crafts. Interior Orientation Parameters (IOPs) to explain physical phenomena of the sensor can be determined through camera calibration (or sensor calibration) (McGlone *et. al.*, 2004; Tsai, 1986; Brown, 1971; Lichti, *et. al.*, 2010; Lichti and Kim, 2011; Rau *et. al.*, 2011).

Geometrical images of the sensor might change time to time due to various physical effects, which indicate thermal influences from the sun in the orbit and vibrations after or during launching the craft. Therefore, the on-orbit sensor calibration is also important after launching. The On-orbit sensor calibration requires a test field of containing different

1) Member, Department of Civil Engineering, Sangmyung University (E-mail: cjkim@smu.ac.kr)

Received 2013. 11. 09, Revised 2013. 11. 14, Accepted 2014. 02. 21

types of variations in heights, and choosing accurate ground control points (Jacobsen *et. al.*, 2005). In fact, although the on-orbit calibration is carried out, it is not easy to accurately determine the sensor's internal orientation parameters, especially in high-resolution satellite sensors (e.g., IKONOS or Quickbird) with narrow Angular Field Of View (AFOV). This is due to the high correlations between the interior and exterior orientation parameters of the sensor (Jacobsen, 2005; Baltsavias and Zhang, 2005). Many researchers have presented the studies about camera calibration, however, the researches about accuracy effects of the internal orientation parameters on the ground are rarely found, especially in three line scanners. For this reason, the study focused on investigation of the IOP bias (especially, focal length bias) effects on the quality of reconstructed object space. This paper will start with the description of three line scanner, which is widely used in photogrammetric field, in Section 2. At next, the paper will geometrically prove the bias including into the focal length, which can have effects on accurate locations of interesting points on the ground. The experimental results and analysis will present on Section 4. Also, during experiments, there were two cases of geo-referencing approaches (i.e., direct and indirect ones). Lastly, the concluding remarks and future work plans are addressed in the last section.

2. Three-Line Scanner System

The three line scanner system, primarily developed by Starlabo Corporation in Tokyo, captures digital image with three different looking angles (Murai, Matsumoto, 2000, Murai, 2001; Chen *et. al.*, 2001). At the same time, the system produced seamless three different digital images. Theoretically, there should be different sets of values for six exterior orientation parameters in each scan line. Therefore, a good trajectory model is necessary for this system. Figure 1 shows a conceptual structure of the sensor, which of one-dimensional scan lines on forward, nadir, and backward. Three scanners with different looking angles share the same perspective center. The MOMS, developed by Germany, and the ADS40, developed by Leica and DLR, can be also classified into three line scanners.

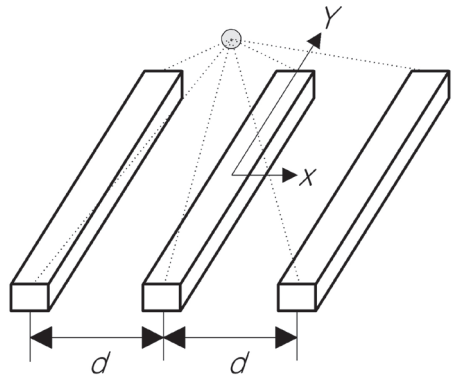

Fig. 1. Three line scanner

An example of images, taken by a three line scanner, is shown in Figure 2. A major advantage of this system is that it can provide images with three different looking angles with almost no time gap between images. Also, unlike with the traditional frame system, the three line geometry is characterized by nearly parallel projection along the flight direction and perspective projection across the flight direction (Gruen and Zhang, 2003).

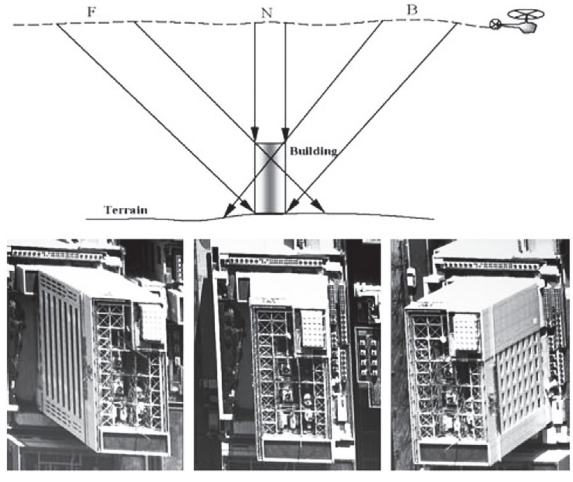

Fig. 2. Forward, nadir, backward images which were taken by a three line scanner, Courtesy of Gruen and Zhang (2003)

3. Geometric Understanding of Focal Length Bias Effects on the Ground

Recall that the interior orientation parameters include the

location of principal point (x_p, y_p, f) and lens distortions. For developing the formula and the level of importance of interior orientation parameters, the focal length among the IO parameters is selected and analyzed by geometrical impact of its bias in a section. The relationship between the IO parameters and EO parameters will be mentioned in later Section 4. Figure 3 indicates three-line scanner with and without a focal length bias, while Figure 4 and 5 are referring shapes in upper direction of a three line scanner with and without bias, respectively.

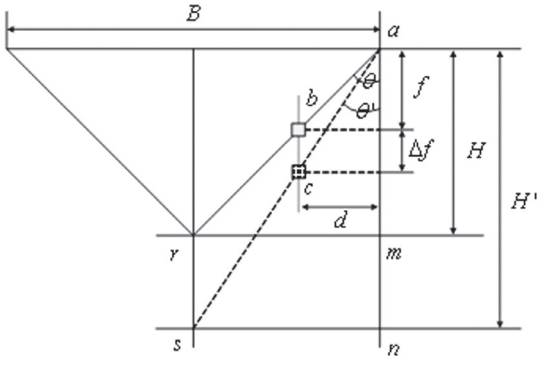

Fig. 3. Side view of three line scanner with and without focal length bias

In Figure 3, *H, B, f*, and *a* present flying height, base distance, focal length, and perspective center, respectively. If there is the bias in amount of Δf in the focal length, an original position of CCD array (i.e., b) changes to the position of *c*, and the position of *r* changes to *s* in the object space.

First of all, we examined the case without any bias through the Figure 4. As seen in the figure, distance between *i* and *j* points was expressed as Equation 1.

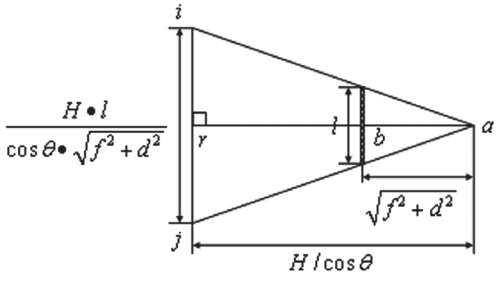

Fig. 4. Top view of three line scanner without focal length bias

$$\overline{ij} = \frac{H \cdot l}{\cos\theta \cdot \sqrt{f^2 + d^2}} = \frac{H \cdot l}{\sqrt{f^2 + d^2}} \times \frac{\tan\theta}{\sin\theta} \quad (1)$$

l indicates the length of CCD array. According to Figure 3, Equation (1) can be modified to Equation (2) by using $\tan\theta = B / 2H$ and $\sin\theta = d / \sqrt{f^2 + d^2}$.

$$\overline{ij} = \frac{H \cdot l}{\sqrt{f^2 + d^2}} \times \frac{\tan\theta}{\sin\theta} = \frac{H \cdot l}{\sqrt{f^2 + d^2}} \times \frac{B}{2H} \times \frac{\sqrt{f^2 + d^2}}{d} = \frac{B \cdot l}{2d} \quad (2)$$

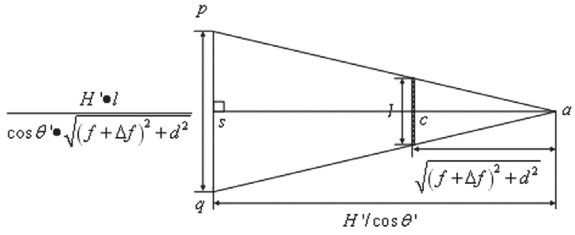

Fig. 5. Top view of three line scanner with focal length bias

As seen in Figure 5, if there is focal length bias in the three line scanner, the distance between points *p* and *q* can be calculated with Equation (3):

$$\overline{pq} = \frac{H' \cdot l}{\cos\theta' \sqrt{(f + \Delta f)^2 + d^2}} = \frac{H' \cdot l}{\sqrt{(f + \Delta f)^2 + d^2}} \times \frac{\tan\theta'}{\sin\theta'} \quad (3)$$

According to Figure 3, Equation (3) can be modified to Equation (4) by using $\tan\theta' = B / 2H'$ and $\sin\theta' = d / \sqrt{(f + \Delta f)^2 + d^2}$:

$$\overline{pq} = \frac{H' \cdot l}{\sqrt{(f + \Delta f)^2 + d^2}} \times \frac{\tan\theta'}{\sin\theta'} = \frac{H' \cdot l}{\sqrt{(f + \Delta f)^2 + d^2}} \times \frac{B}{2H'} \times \frac{\sqrt{(f + \Delta f)^2 + d^2}}{d} = \frac{B \cdot l}{2d} \quad (4)$$

From Equations (2) and (4), the distance ($\overline{ij}$) between point *i* and *j*, and the distance ($\overline{pq}$) between point *p* and *q* are determined to be same by $\frac{B \cdot l}{2d}$.

On the other hand, $H = \frac{f \cdot B}{2d}$ and $H' = \frac{(f + \Delta f) \cdot B}{2d}$ can be derived from Figure 3 by using triangle similarity. Thus, the value $H' - H$ is same as $\frac{\Delta f \cdot B}{2d}$.

From the above variations, we were able to find that the focal length bias does not have effects along and across scan lines in three line scanner, however, there were some effects in accuracies of the vertical direction.

4. Experimental Results and Analysis

This study evaluated accuracies of direct and indirect geo-referencing for a three line scanner, by changing the amounts of the focal length biases. In the study of direct geo-referencing, external orientation parameters were set as true values for investigating the bias effects only.

Table 1 shows the specific experimental conditions of sensor trajectory, image measurement error, control information, accuracy of Global Positioning Systems (GPS), accuracy of Inertial Navigation Systems (INS), accuracy of Ground Control Points (GCP), and height variation of GCP. 100 Ground Control Points (GCPs) were created by changing the altitude of ±500m. GPS accuracies of high altitude are 4cm for all X, Y, Z directions, and also accuracies of low altitude are 15cm for all directions. INS accuracies of high altitude were 7 seconds, but 15 seconds for low altitude case. When indirect geo-referencing were performed, 10 GCPs, among the 100 GCPs, were used for sensor modeling, and others were used for Check Points (CP). Since direct geo-referencing did not require any of GCPs, all 100 GCPs were used as check points.

Table 1. Experimental conditions for generating the synthetic data

Item		Contents
Sensor trajectory Image measurement error Control Information		1st order polynomial equation 1 pixel GPS/INS or GCP
Direct geo-referencing	Accuracy of GPS	High altitude: 0.04m(X), 0.04m(Y), 0.04m(Z)
		Low altitude: 0.15m(X), 0.15m(Y), 0.15m(Z)
	Accuracy of INS	High altitude: 7″(ω), 7″(φ), 12″(κ)
		Low altitude: 15″(ω), 15″(φ), 20″(κ)
Indirect geo-referencing	Accuracy of GCP	0.04m(X), 0.04m(Y), 0.04m(Z)
Height variation	± 500m	

Table 2 shows information about high and low altitude sensors and amounts of IOP biases. The simulation of high altitude space-borne was based on IKONOS, while the low altitude scanner case was based on ADS40 sensor information. A flying height of three line of a high altitude sensor is 680km above ground. The focal length is 10m in both forward and backward directions, which is 8.98794 m for the nadir case. At this point, noted that the focal lengths in nadir direction and in off-nadir cases (i.e., forward and backward directions) are different, but they have the same perspective center. Please, refer to Figure 1 for clear understanding.

The Ground Sampling Distance (GSD) is 0.68m. The amount of principal point bias is around 50um. Also, the range of focal length bias is from 50um to 50,000um.

In the case of low altitude, the flying height is 5,500m above the ground. Focal length is 75mm in both forward and backward directions, and 67.40955mm for the nadir direction. The Ground Sampling Distance (GSD) is 0.73m. The amount of principal point bias is around 0.375um. Also, the range of focal length biases is from 0.375um to 375um.

Table 2. Specifications and the amounts of bias in both low and high altitude sensors

Category		Three line
High altitude	Flying height(m)	680,000
	Pixel size (㎛)	10
	x_p (mm)	0
	y_p (mm)	0
	f (mm)	8,987.94 (nadir), 10,000 (forward & backward)
	Mean GSD(m)	0.68
	Amount of bias	50㎛ ($\triangle x_p$, $\triangle y_p$), 50㎛ ~ 50,000㎛ ($\triangle f$)
Low altitude	Flying height(m)	5,500
	Pixel size (㎛)	10
	x_p (mm)	0
	y_p (mm)	0
	f (mm)	67.40955 (nadir), 75 (forward & backward)
	Mean GSD(m)	0.73
	Amount of bias	0.375 ㎛ ($\triangle x_p$, $\triangle y_p$), 0.375 ㎛ ~ 375 ㎛ ($\triangle f$)

4.1. Focal Length Bias Effects In the Case Of Direct Geo-referencing

Tables 3 and 4 display results for the direct geo-

referencing with high and low altitudes, respectively. In direct orientation, the achieved accuracy is significantly affected by the bias in internal orientation parameters, as seen in the experiments H_A1 to H_A4, L_A1 to L_A4. There is an error between 3.8 and 4.0m approximately across the san lines (X-direction) by adding the bias into x_p in the high altitude case(the experiments from H_A1 to H_A4), while there is about 3.8m error in the scan line (Y-direction) by adding the bias into y_p. As the bias values in the focal length increase, RMSE along the Z-direction increases proportionally, which has been proven mathematically in Section 3. In fact, this phenomena also occurs similar in low altitude cases (the experiments from L_A1 to L_A4). Figure 6 and 7 illustrate the visual understanding of effects from the focal length bias. As seen in figures, relationship between the focal length bias and the RMSE along Z direction is almost perfect linear for both high and low altitudes three line scanners. The Pearson's correlation coefficients between the two variables in both high and low altitudes were 1 and more than 0.999, respectively.

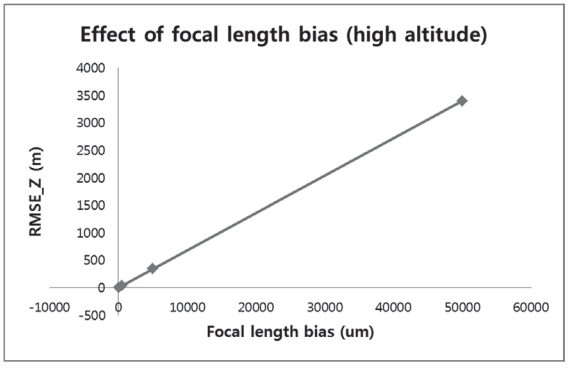

Fig. 6. Effects of focal length bias in high altitude ($R^2 = 1$)

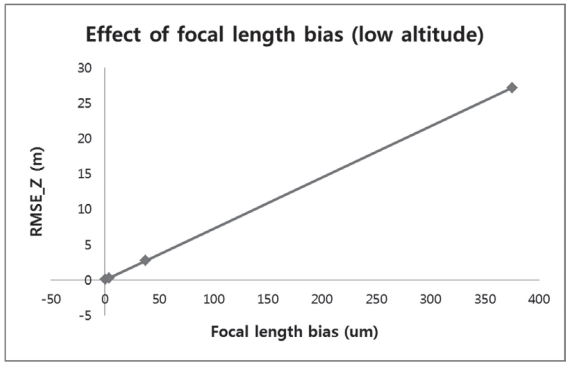

Fig. 7. Effects of focal length bias in low altitude ($R^2 > 0.999$)

Table 3. High altitude three line scanner (direct geo-referencing)

Exp	Type	IOP Bias(um)			GCP	CP	$\hat{\sigma}_0$	RMSE(m)				
		Δx_p	Δy_p	Δf				X	Y	Z	XY	XYZ
H_A1	Direct	50	50	50	0	100	0.0006	3.77	3.78	3.40	5.34	6.33
H_A2				500			0.0055	3.77	3.78	34.00	5.34	34.41
H_A3				5000			0.0552	3.79	3.78	339.96	5.35	340.01
H_A4				50000			0.5519	4.00	3.78	3399.63	5.50	3399.64

Table 4. Low altitude three line scanner (direct geo-referencing)

Exp	Type	IOP Bias(m)			GCP	CP	$\hat{\sigma}_0$	RMSE(m)				
		Δx_p	Δy_p	Δf				X	Y	Z	XY	XYZ
L_A1	Direct	0.375	0.375	0.375	0	100	0.0001	0.71	0.05	0.06	0.71	0.72
L_A2				3.75			0.0001	0.71	0.05	0.26	0.71	0.76
L_A3				37.5			0.0003	0.69	0.05	2.70	0.70	2.79
L_A4				375			0.0039	0.54	0.05	27.19	0.54	27.20

4.2. Focal Length Bias Effects In the Case Of Indirect Geo-referencing

On the other hand, the effects of IOP biases are insignificant on the reconstructed object space for indirect geo-referencing according to Tables 5 and 6 from H_A5 to H_A8 and L_A5 to L_A8. This result was expected because EOP changes to compensate for the IOP biases. In other words, derived attitudes and positions of the scanner absorbed effects from IOP biases. Most of the RMSE values in the experiments from H_A5 to H_A8 are close to zeroes, since we deal with a scanner of a narrow Angular Field of View (AFOV) and a high flying height. In this case, internal orientation parameters correlate with external orientation parameters. All relevant experiments, except for L_A8 (i.e., L_A5 to L_A7) of low-altitude scanner, also had the RMSE values close to zeroes. A reason for the result of L_A8 is that attitudes and positions of the scanner do not absorb all effects from IOP biases comparing to the high-altitude scanner, when the scanner does not have narrow AFOV. Habib *et. al.* (2007) has addressed the relationship of AFOV and correlation between IOP and EOP. For more detailed information, please refer to Habib *et. al.* (2007).

Table 5. High altitude three line scanner (indirect geo-referencing)

Exp	Type	IOP Bias(um)			GCP	CP	$\hat{\sigma}_0$	RMSE(m)				
		Δx_p	Δy_p	Δf				X	Y	Z	XY	XYZ
H_A5	Indirect	50	50	50	10	90	0.0000	0.02	0.04	0.03	0.04	0.05
H_A6				500			0.0000	0.02	0.04	0.03	0.04	0.05
H_A7				5000			0.0000	0.02	0.04	0.03	0.04	0.05
H_A8				50000			0.0000	0.02	0.04	0.03	0.04	0.05

Table 6. Low altitude three line scanner (indirect geo-referencing)

Exp	Type	IOP Bias(m)			GCP	CP	$\hat{\sigma}_0$	RMSE(m)				
		Δx_p	Δy_p	Δf				X	Y	Z	XY	XYZ
L_A5	Indirect	0.375	0.375	0.375	10	90	0.0000	0.00	0.00	0.00	0.00	0.00
L_A6				3.75			0.0000	0.00	0.02	0.00	0.02	0.02
L_A7				37.5			0.0003	0.02	0.16	0.02	0.16	0.16
L_A8				375			0.0026	0.17	1.56	0.19	1.57	1.58

Table 7. Correlation matrix of the IO and EO parameters (absolute values)

	x_p	y_p	f	X_0	Y_0	Z_0	ω	φ	κ
x_p	1	0.10	0.11	0.23	0.16	0.23	0.10	0.54	0.10
y_p	0.10	1	0.39	0.39	0.66	0.39	0.99	0.37	0.99
f	0.11	0.39	1	0.99	0.90	0.99	0.40	0.89	0.40
X_0	0.23	0.39	0.99	1	0.90	0.99	0.40	0.94	0.40
Y_0	0.16	0.66	0.90	0.90	1	0.90	0.67	0.83	0.75
Z_0	0.23	0.39	0.99	0.99	0.90	1	0.40	0.80	0.40
ω	0.10	0.99	0.40	0.40	0.67	0.40	1	0.30	0.99
φ	0.54	0.37	0.89	0.94	0.83	0.80	0.30	1	0.32
κ	0.10	0.99	0.40	0.40	0.75	0.40	0.99	0.32	1

We also carried out the correlation analysis to figure out which IO parameters and EO parameters are coupled under different strength levels. Table 7 indicates a correlation matrix of IO and EO parameters. According to the table 7, x_p is somewhat correlated with φ(rotation along Y-axis). The table also refers that y_p is strongly correlated with ω (rotation along X-axis) and κ(rotation along Z-axis) as well as it is somewhat correlated with Y_0 (translation along Y-direction). For f, it is strongly correlated with X_0 (translation along X-direction) and Z_0 (translation along Z-direction). Also, it is somewhat correlated with Y_0 and φ. In fact, some of the EO parameters are strongly correlated with each other, such as X_0 & Z_0 and ω & κ.

5. Concluding Remarks and Future Work

In this study, the effects of focal length bias on the coordinates of the reconstructed objects were mainly analyzed for three line scanners in space-borne (i.e., high altitude) and airborne (i.e., low altitude). This research applied two different geo-referencing approaches, which are direct and indirect ones. The accuracy of the reconstructed object space for analyzing the bias effects was evaluated by adding artificial biases to the principal point and focal length. Based on the real trajectory of sensors, a topography of the object space was simulated, and trajectories of sensors were also determined. Firstly, one of the focal length bias effects was proven through mathematical derivations. As more experiments were carried out, those results also showed the similar trends to one that is proven through mathematical proofs. In fact, IOP biases of the direct geo-referencing generated serious errors on determination of three-dimensional coordinates; as the bias value in the focal length increases, error along the vertical direction increases proportionally. The Pearson's correlation coefficients, in which between the focal length biases and the RMSE values along the vertical direction, showed 1 and more than 0.999 for the high and low altitude cases, respectively.

On the other hand, the effects of IOP biases are insignificant on the reconstructed object space, when indirect geo-referencing is carried out. In this case, the derived attitudes and positions of the scanner absorbed the effects from the biases. Similar phenomena occur for the low altitude experiments. However, when the amount of the bias is very large, the attitudes and positions of the scanner do not absorb all the effects from the bias. Additionally, the correlation analysis is carried out, and the correlation between the IO and the EO parameters are proven as well.

Simulated data was used for this study due to difficulties in data acquisition of the IOP bias, however, future research will be better to concentrate on analysis of the bias effects with real data. Moreover, the terrain roughness effects in case of low altitude scanner will be studied in the future research.

Acknowledgment

This study was supported by the intramural research funds from SANGMYUNG University, 2012.

References

Baltsavias, E., Zhang, L., and Eisenbeiss, H. (2005), DSM Generation and interior orientation determination of IKONOS images using a test field in Switzerland, *ISPRS Hannover Workshop 2005 on High-Resolution Earth Imaging for Geospatial Information*, 17-20 May, Hannover, Germany(on CD-ROM).

Brown, D. (1971), Close range camera calibration, *Photogrammetric Engineering*, Vol. 37, No. 8, pp. 855-866.

Chen, T., Shibasaki, R., and Morita, K. (2001), High precision georeference for airborne three-line scanner (TLS) Imagery. *3rd International Image Sensing Seminar on New Developments in Digital Photogrammetry*, Sept. 24-27, Gifu, Japan, pp. 71-82.

Fraser, C., Baltsavias, E. P., and Gruen, A. (2002), Processing of IKONOS imagery for sub-meter 3D positioning and building extraction, *ISPRS Journal of Photogrammetry & Remote Sensing*, 56(3), pp. 177-194.

Gruen, A., and Zhang, L. (2003), Sensor modeling for aerial triangulation with three-line-scanner (TLS) imagery, *Photo-grammmetrie, Fernerkundung, Geoinformation*

(PFG), No. 2, pp. 85-98.

Habib, A., Shin, S., Kim, K., Kim, C., Bang, K., Kim, E., and Lee, D. (2007), Comprehensive analysis of sensor modeling alternatives for high resolution imaging satellites, Vol. 73, No. 11, pp. 1241-1251.

Jacobsen, K. (2005), Geometry of satellite images–calibration and mathematical models, *Korean Society of Remote Sensing*, *ISPRS International Conference*, Korea, Jeju, pp. 182-185.

Jacobsen, K., Büyüksalih, G., and Topan, H. (2005), Geometric models for the orientation of high resolution optical satellite sensors, *International Proceedings of ISPRS Annual Convention*, Vol. XXXVI 1/W3. Hannover, CD-ROM.

Lee, C., and Bethel, J. (2004), Extraction, modelling, and use of linear features for restitution of airborne hyperspectral imagery, *ISPRS Journal of Photogrammetry & Remote Sensing*, Vol. 58, pp. 289-300.

Lichti, D. D., Kim, C., and Jamtsho, S. (2010), An integrated bundle adjustment approach to range camera geometric self-calibration, *ISPRS Journal of Photogrammetry and Remote Sensing*, Vol. 65, No. 4, pp. 360-368.

Lichti, D. D., and Kim, C. (2011), A comparison of three geometric self-calibration methods for range cameras, *Remote Sensing*, Vol. 3, No. 5, pp. 1014-1028.

McGlone, C., Mikhail, E., and Bethel, J. (2004), *Manual of photogrammetry, 5th Edition*, ASPRS, pp. 215-216.

Murai, S. (2001). Development of helicopter-borne three line scanner with high performance of stabilizer and IMU. *3rd International Image Sensing Seminar on New Developments in Digital Photogrammetry*, Sept. 24-27, Gifu, Japan, pp. 1-3.

Murai, S., and Matsumoto, Y. (2000), The development of airborne three line scanner with high accuracy INS and GPS for analyzing car velocity distribution. *IAPRS*, Vol.33, Part B2, Amsterdam, pp. 416-421.

Rau, j., Habib, A., Kersting, A., Chiang, K., Bang, K., Tseng, Y., and Li, Y. (2011), Direct sensor orientation of a land-based mobile mapping system, *Sensors*, Vol. 11, No. 7, pp. 7243-7261.

Tsai, R. (1986), An efficient and accurate camera calibration technique for 3D machine vision, *In: Proc. IEEE Computer Vision and Pattern Recognition Conference*, pp. 364–374.